

An Automated Scheme for the Large-Scale Survey of Herbig-Haro Objects

LICAI DENG,^{1,3,4,5} JI YANG,^{2,3,4} ZHONGYUAN ZHENG,^{1,3,4} AND ZHAOJI JIANG^{1,3,4}

Received 2000 December 3; accepted 2001 January 8

ABSTRACT. Owing to their spectral properties, Herbig-Haro (HH) objects can be discovered using photometric methods through a combination of filters, sampling the characteristic spectral lines and the nearby continuum. The data are commonly processed through direct visual inspection of the images. To make data reduction more efficient and the results more uniform and complete, an automated searching scheme for HH objects is developed to manipulate the images using IRAF. This approach helps to extract images with only intrinsic HH emissions. By using this scheme, the pointlike stellar sources and extended nebulous sources with continuum emission can be eliminated from the original images. The objects with only characteristic HH emission become prominent and can be easily picked up. In this paper our scheme is illustrated by a sample field and has been applied to our surveys for HH objects.

1. INTRODUCTION

Herbig-Haro (HH) objects are one of the major manifestations of mass outflow activities from young stellar objects (e.g., Reipurth & Raga 1999). These shock-excited objects exhibit low-excitation emission lines in the optical spectral range with little or even no continuum component (Schwartz 1975, 1978). The most prominent lines of an HH spectrum include [O I] $\lambda\lambda 6300, 6363$; [N II] $\lambda\lambda 6548, 6584$; H α $\lambda 6563$; [S II] $\lambda\lambda 6717, 6731$, and so on.

HH objects can be found by broadband imaging, such as in *V*, *R*, and *I*, combined with spectroscopic confirmation based on the identification of their characteristic emission-line spectra (e.g., Mundt, Ray, & Raga 1991). Photometric methods have also been widely used in the search of HH objects. Earlier approaches included visual inspection of survey plates (e.g., Gyulbudaghian, Glushkov, & Denisyuk 1978; Cohen 1980; Reipurth 1981). Improved methods, typically a [S II] narrowband filter combined with a red continuum filter, were also used to search for HH candidates (e.g., Reipurth & Graham 1988; Ogura 1990; Mader et al. 1999). In these cases, two filters were employed, with one sampling the emission lines, such as H α or the forbidden lines of [S II] at $\lambda\lambda 6717, 6731$, and the other sampling the adjacent line-free continuum. Through the line filter, the characteristic lines of HH objects appear, while in the line-free band, only continuum emission can be seen. There-

fore, a bona fide HH object should appear prominently in the line filter band but not in the continuum band.

A refined approach was achieved by large-field CCD imaging with properly selected intermediate- to narrowband filters which transmit or exclude the characteristic HH lines (Yan et al. 1998, hereafter Paper I; Zhao et al. 1999, hereafter Paper II). In these surveys, two sets of CCD images were taken, with one set to sample the strong emission lines using a narrowband filter and the other set to acquire the adjacent continuum using an intermediate-band filter, as reported in detail in Papers I and II. Candidate HH objects can then be picked up by manipulation of the two images. We have started surveys for HH objects using the same telescope and CCD camera for the BATC⁶ multicolor sky survey. The BATC survey uses 15 intermediate-band filters covering 3000–10000 Å. One of the filters, BATC[09], covers the strong emission lines of HH objects, including [N II] $\lambda\lambda 6548, 6584$; H α $\lambda 6563$; and [S II] $\lambda\lambda 6717, 6731$. Another filter, BATC[10], samples the red continuum side of the lines. Thus, BATC[09] covers especially the H α line, which makes it difficult to avoid possible contamination of the results by other kinds of emission-line objects such as H II regions or planetary nebulae. For this reason, we utilize a narrowband filter covering only the [S II] lines. This latter filter plus the BATC[10] form the present photometry system in our HH survey (see Paper II for details).

As a survey project, BATC has created a set of tools to process its CCD data in a pipeline mode, including bias and overscan subtraction, flat-fielding, and coordinating. However, HH survey data cannot be processed in the same way as BATC data. After normal CCD data prerduction, our images have to be reduced separately. We built additional procedures based on

¹ Beijing Astronomical Observatory, Chinese Academy of Sciences, Beijing 100012, China.

³ BAC: Chinese Academy of Sciences–Peking University Joint Beijing Astrophysical Center.

⁴ Chinese National Astronomical Observatories, Chinese Academy of Sciences, A20 Datun Road, Chaoyang District, Beijing 100012, China.

⁵ denglicai@china.com.

² Purple Mountain Observatory, Academia Sinica, Nanjing 210008, China.

⁶ BATC: Beijing-Arizona-Taiwan-Connecticut Multicolor Sky Survey. See Chen (1994) for the setup of the BATC program.

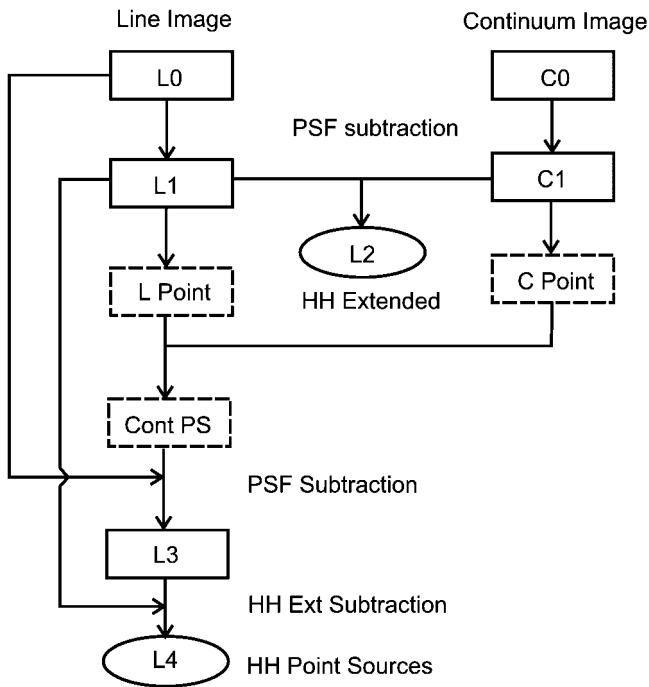


FIG. 1.—Schematic flowchart of the automated procedure. The solid line boxes denote the raw and intermediate images, dashed line boxes are tables of the point sources, and ellipses are the output images of the automated scheme. L1 and C1 are the residual images coming from the normal PSF fitting photometry which also creates the catalogs of point sources, L Point and C Point. The table of common point sources is made by a comparison between the two catalogs. L0 is processed twice with PSF fitting: first, subtracting off all point sources, giving the residual image L1; second, subtracting the common point sources of the two original images L0 and C0, giving the residual image L3. L2 is the result of subtracting C1 from L1. L4 is derived by subtracting L3 from L1.

IRAF.⁷ This paper introduces the methodology used in the procedures along with an example. In § 2, we give a description of the methodology. An example of image processing using the method is given in § 3.

2. METHODOLOGY

Morphologically, HH objects can be either extended and nebulous objects or pointlike, compact objects, depending on their intrinsic structure as well as the sensitivity of observation. In practice, it is a useful concept to divide the HH objects into extended objects and pointlike objects and to consider them separately.

Normal stellar sources in our images are thought of as contamination, which makes identification of HH objects difficult. Within IRAF we can eliminate such contamination using the point-source photometry utility DAOPHOT II (Stetson 1987).

However, for a large amount of data, it is too strenuous to follow the interactive procedure. The key element for doing point-source subtraction is the point-spread function (PSF) star selection. We used an automated PSF selection program developed by BATC (Zheng 1998),⁸ which is coded in FORTRAN and can be invoked in IRAF. By using such an automated PSF star selection code, we can integrate all the DAOPHOT II and image algorithmic tasks to get the clean images. For point-source photometry of BATC images, a clone of DAOPHOT II named PIP2 was developed, which does the same task as DAOPHOT II in noninteractive mode, taking advantage of the automatic PSF star selection code. PIP2 can be invoked within IRAF.

IRAF is one of the most popularly used data reduction software packages and has been one of the standard platforms for astrophysical data reduction including CCD image processing. The CL script language within IRAF allows advanced programming of the individual tasks for different purposes. In Paper I, our images were reduced using IRAF interactively. That was a purely “visual” work in which one had to fasten one’s eyes on the screen of two blinking images over a long time in order to pick up any HH candidates. The work was rather exhaustive, but that was not the only problem. Direct visual inspection of the images is certainly less objective and could cause other problems such as possibly missing candidates. For a survey program, completeness and uniformity are the most important issues to consider. To achieve this goal we have made the following automated scheme within IRAF to get two final images, one for the point sources and the other for extended sources; both are free of continuum contamination.

It is clear from § 1 that HH object searching by CCD photometry is the manipulation of two images directly acquired by observation: (1) the image taken using the filter [S II] labeled as L0, which covers the characteristic lines of HH objects; and (2) the image sampling the adjacent continuum of the same field of view labeled as C0. Our primary motivation is to eliminate all the background emission and to get images with only HH emission. The technical flowchart is given in Figure 1. The whole process can be divided into the following steps:

1. The first step is to process the two images, L0 and C0, using the automated point-source subtraction task PIP2. This step gives a catalog of point sources for each image and a corresponding output image with all point sources subtracted. The leftover residual images are extended sources. We name the output image for L0 as L1 and that of C0 as C1. L1 and C1 are intermediate data for the next steps.

2. The second step is to get an image containing only the extended emission-line sources. Following step 1, we know that L1 contains *all* the extended sources, while C1 contains *only* the extended continuum sources. So, directly subtracting

⁷ IRAF is the Image Reduction and Analysis Facility, written and supported by the IRAF programming group at the National Optical Astronomy Observatories (NOAO) in Tucson, Arizona.

⁸ See also Z. J. Jiang 1999, <ftp://jets.pmo.ac.cn/pub/tools/HHsearch>.

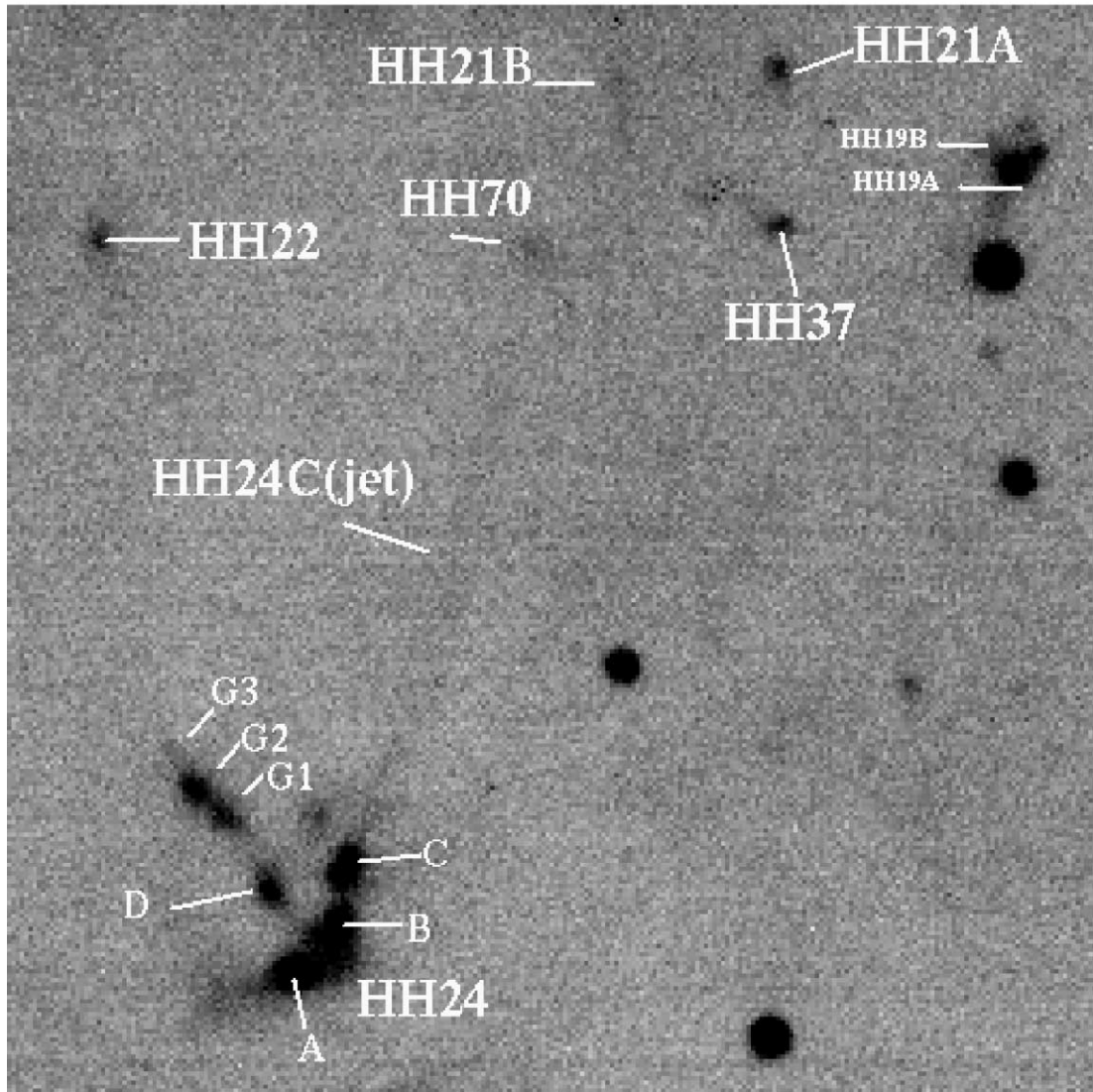


FIG. 2.—Subframe [S II] image from an HH survey field in the NGC 2068/2071 region. The image size is 512×512 pixels. The HH complex HH 24 is located in the lower left, with all its members labeled. The upper part shows some other objects (see a short description in § 3).

C1 from L1 creates exactly what we need, the HH extended images. We call the resulting image L2.

3. The two catalogs given in step 1 are apparently different. It is clear that all kinds of point sources should appear in the catalog “L Point” because the filter covers the emission lines from the HH objects and at the same time also includes the continuum for normal stellar or pointlike sources. In the catalog “C Point,” however, only the point sources with continuum show up. The HH objects do not appear because they have almost no continuum in that passband. In this step, we make a table, “Cont PS,” of sources which are common in the two catalogs. Subtracting the common point sources from the image L0 defines an image L3. L3 contains not only the point emission-line sources but also the extended sources in both continuum and emission lines.

4. To get an image with only the emission-line point sources, we can simply subtract off all these extended sources from the image. So another image containing only the extended sources for the same field is needed, and L1 is exactly such an image. Therefore, subtracting L1 from L3 gives us a clean image of HH point sources. Within IRAF, this is straightforward. The output image is noted as L4.

L2 and L4 are the two final images. With all the continuum sources stripped off from the images, sources with characteristic HH emission stand out sharply. Searching for the HH candidates now occurs directly from the static images of L2 and L4. It worth emphasizing that there is no loss of information about the HH objects throughout the scheme of image reduction. Any

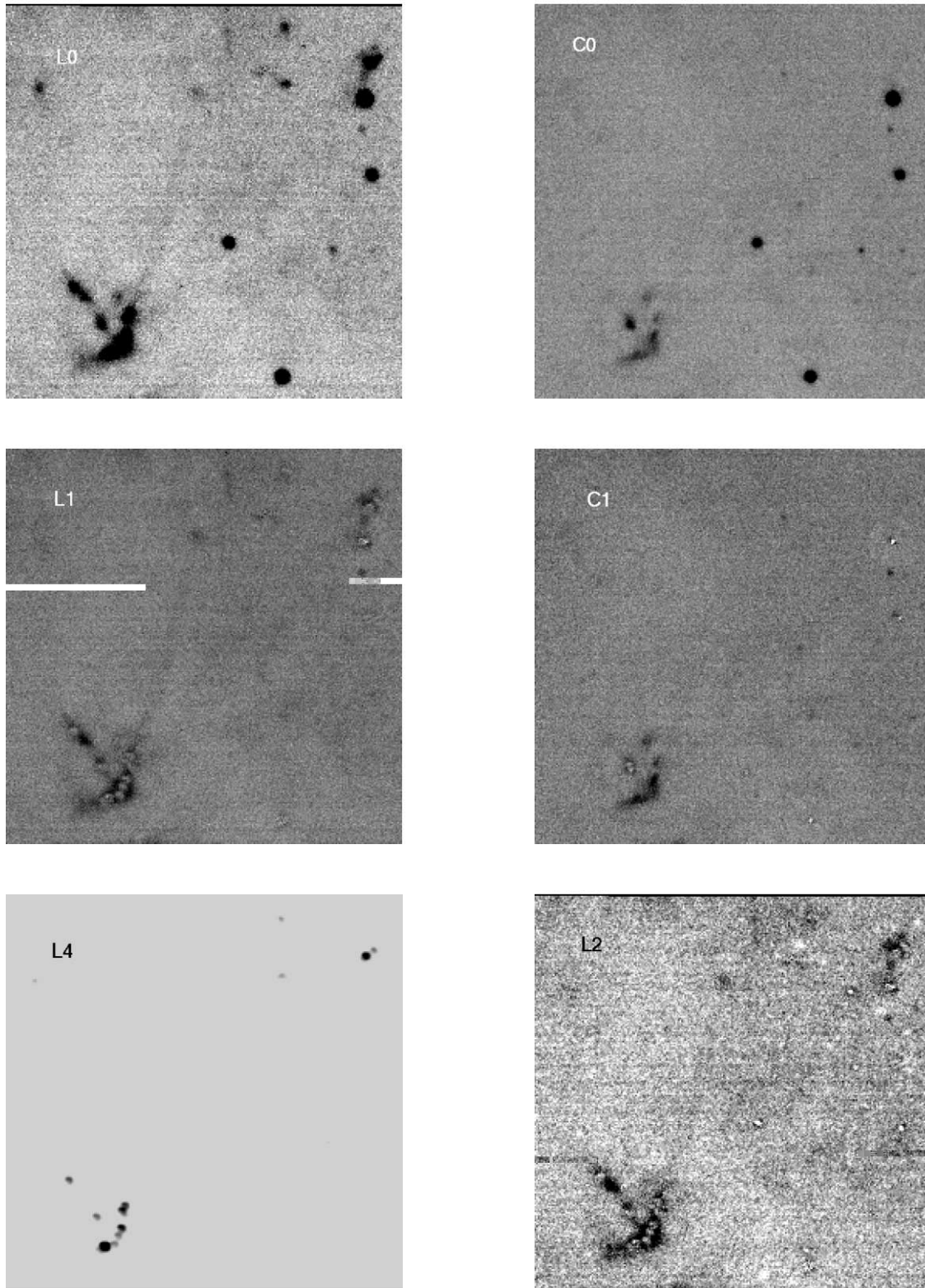


FIG. 3.—Images showing the step-by-step procedure of image manipulation. L0 and C0 are the original images in HH characteristic line region and adjacent continuum, respectively. L1 and C1 are the two intermediate images with point sources subtracted off for L0 and C0. L4 is the output image for the pointlike HH sources. L2 is the output image for the extended HH sources.

object on the original images with characteristic HH emission, either extended or pointlike, should be present on one of the two final images. As the identification of the objects is basically made on the morphology on the original images, very careful visual inspection of both the working images (L2 and L4) and the original images (L0 and C0) is still needed. We always double-check the results by different people at the visual inspection stage, in order to guarantee the completeness of the results.

In light of the above methodology, a set of tools written in CL was developed for HH image processing.⁹ A detailed description of the procedure and the CL tasks is presented by Zhao (1999).

3. A SAMPLE FIELD

The automated HH search utility has been applied in searching targets in a 1 field of view covering NGC 2068 and NGC 2071 (Paper II). There is a rich HH object complex in our program field, containing HH 24 (Mundt et al. 1991), HH 22 (Herbig 1974), HH 70, HH 21A and B, HH 37, and HH 19 (Eislöffel & Mundt 1997). These HH objects cover various morphological types. Therefore we have adopted this complex as an example to show how the scheme works. A subframe of our field is used to show the image processing procedure (see the [S II] subimage in Fig. 2). The size of the subframe is 512×512 pixels, corresponding to about $30' \times 30'$. As illustrated, there are several pointlike knots, HH 24A, B, and C of the HH24 complex in the southeast and HH 19A in the northwest of the field. HH 24C and HH 24C-jet form a long jet which is clearly visible in this raw image.

Figure 3 shows the original, intermediate, and resultant images following the automated searching procedure. Panels L0 and C0 are, respectively, the original [S II] image sampling HH characteristic lines and the BATC[10] image for the nearby continuum. L1 and C1 are the corresponding images with all point sources subtracted. The results of the whole procedure are the two final images L2 and L4, containing the extended and pointlike HH sources. By subtracting the point sources using the automatic task PIP2, the background stellar images are eliminated from images L0 and C0. In panel L1, the pointlike HH objects HH 24A, B, C, D, G2, HH 19A, and the cores of HH 21A and HH 37 all disappear. Panel C1 is a clean image containing only extended sources in the continuum, with little

contamination from the wings of bright stars. This is a typical residual image created by task PIP2. According to the methodology and the flowchart in Figure 1, the point HH sources can be found by subtracting the common point sources from the [S II] image (i.e., panel L0, then subtract panel L1 from the residual images, which gives the final image for point-source panel L4). This is a very clear image for pointlike HH sources in which, if compared with Figure 2, all the pointlike HH objects are prominent. Panel L2 is an image showing only the extended HH sources, which is made by subtracting C1 from L1, following step 4 in § 2. Again, we see only the extended sources on this image, such as the jet HH 24C-jet.

We have made a series of survey observations of HH objects in the nearby star-forming regions, such as the NGC 1333/B1 region (Paper I), the NGC 2068/2071 region (Paper II), the L1641 region (Wang et al. 2000; Yang & Yao 2000), the L1536 region (Wang et al. 2001), and the ρ Oph region (J. Wu et al. 2001, in preparation). So far, a total of 34 HH objects have been discovered and numbered along with a number of potential HH candidates. In all these surveys except that introduced in Paper I, we have applied the current automated scheme to process the large-field images and to pick out HH candidates. The application of this method significantly improved the working efficiency and completeness of the surveys.

4. CONCLUSION

An automated scheme has been designed to reduce the CCD images taken from the large-scale surveys for HH objects. Pipeline packages based on this scheme have been built using the IRAF package to realize the procedure. By eliminating continuum sources, this scheme picks up two static images containing the HH extended and HH pointlike sources, respectively. This scheme is a useful method to derive the HH-specific images which can be used in the search for HH objects. This results in a significant improvement of both efficiency and uniformity, as was proved by a series of surveys for HH objects in the local star-forming regions.

The authors would like to thank our colleagues at Beijing Astronomical Observatory for their help with the observations. We are indebted to Hongchi Wang and Min Wang for interesting discussions and to the latter for preparing the figures used in this paper. This work is supported by the Natural Science Foundation of China through grants 19625307 and 19603002 and the Ministry of Science and Technology through grant G19990754.

⁹ All the scripts and the FORTRAN code for automated PSF star selection can be found at <ftp://jets.pmo.ac.cn/pub/tools/HHsearch>.

REFERENCES

- Chen, J. S. 1994, in IAU Colloq. 148, Future Utilization of Schmidt Telescopes, ed. J. Chapman, R. Cannon, S. Harrison, & B. Hidayat (ASP Conf. Ser. 84; San Francisco: ASP), 30
 Cohen, M. 1980, AJ, 85, 29
 Eislöffel, J., & Mundt, R. 1997, AJ, 114, 280
 Gyulbudaghian, A. L., Glushkov, Yu. L., & Denisyuk, E. K. 1978, ApJ, 224, L137
 Herbig, G. H. 1974, Lick Obs. Bull. 658

- Mader, S. L., Zealey, W. J., Parker, Q. A., & Mashedier, M. R. W. 1999, *MNRAS*, 310, 331
- Mundt, R., Ray, T. R., & Raga, A. C. 1991, *A&A*, 252, 740
- Ogura, K. 1990, *PASP*, 102, 1366
- Reipurth, B. 1981, *A&AS*, 44, 379
- Reipurth, B., & Graham, J. A. 1988, *A&A*, 202, 219
- Reipurth, B., & Raga, A. C. 1999, in *The Origin of Stars and Planetary Systems*, ed. C. J. Lada & N. D. Kylafis (Dordrecht: Kluwer), 267
- Schwartz, R. D. 1975, *ApJ*, 195, 631
- . 1978, *ApJ*, 223, 884
- Stetson, P. B. 1987, *PASP*, 99, 191
- Wang, H., Yang, J., Wang, M., Deng, L., Yan, J., & Chen, J. 2001, *AJ*, in press
- Wang, M., Zhao, B., Yang, J., Deng, L., & Chen, J. 2000, *Chinese Phys. Lett.*, 17, 304
- Yan, J., Wang, H., Wang, M., Deng, L., Yang, J., & Chen, J. 1998, *AJ*, 116, 2438 (Paper I)
- Yang, J., & Yao, Y. 2000, in *IAU Symp. 197, Astrochemistry: From Molecular Clouds to Planetary Systems*, ed. Y. Minh & E. van Dishoeck (San Francisco: ASP), 213
- Zhao, B. 1999, Master's thesis, Beijing Astron. Obs.
- Zhao, B., Wang, M., Yang, J., Wang, H., Deng, L., & Chen, J. 1999, *AJ*, 118, 1347 (Paper II)
- Zheng, Z. Y. 1998, Ph.D thesis, Beijing Astron. Obs.